Kinetics and Catalysis, Vol. 45, No. 4, 2004, pp. 607–617. Translated from Kinetika i Kataliz, Vol. 45, No. 4, 2004, pp. 642–653.

Porous Al_2O_3/Al Metal Ceramics Prepared by the Oxidation of Aluminum Powder under Hydrothermal Conditions Followed by Thermal Dehydration: IV. Effect of Oxide Additives on the Composition and Texture Characteristics of MO_x/Al_2O_3/Al Composites

S. F. Tikhov, Yu. V. Potapova, V. B. Fenelonov, V. A. Sadykov, A. N. Salanov, S. V. Tsybulya, and L. F. Mel'gunova

Boreskov Institute of Catalysis, Siberian Division, Russian Academy of Sciences, Novosibirsk, 630090 Russia

Received December 16, 2002

Abstract—The synthesis, structure, and texture of metal ceramics based on Al_2O_3/Al with powdered oxide additives (CaO, MgO, Al_2O_3, La_2O_3, and TiO_2) were studied. Analytic expressions were derived to relate the main macroscopic characteristics of the composites.

INTRODUCTION

Previously [1–3], the results of studies on the synthesis and properties of Al_3O_3/Al composites prepared by the hydrothermal oxidation of aluminum followed by thermal decomposition in air were reported. The more complex catalytic composites Co_3O_4/Al_2O_3/Al and $MZrO_y/Al_2O_3$/Al (M = Ca, Sr, or Ba), which were prepared by the encapsulation of powdered oxides in an Al_2O_3/Al matrix upon hydrothermal oxidation and calcination, were also studied [4]. However, the effect of additives on the process of oxidation and the texture characteristics of the resulting composites was not studied in detail. A study of the genesis of a number of model composites like MO_x/Al_2O_3/Al, which contained oxides that are common promoters for catalysts and supports (CaO, MgO, Al_2O_3, La_2O_3, and TiO_2), revealed the nonadditive effects of the dopants both at the stage of hydrothermal oxidation and in the course of thermal decomposition [5]. The aim of this work was to evaluate quantitatively the effect of oxide dopants on the textural and mechanical properties of Al_2O_3/Al metal ceramics.

EXPERIMENTAL

Aluminum powder of PA-4 grade was used as a starting material for the preparation of an Al_2O_3/Al matrix. Metal oxides were prepared by the thermal decomposition of corresponding nitrates of analytical grade at 700°C. The CaO was additionally ground. Powdered γ-Al_2O_3 of A-1 grade was used as an aluminum oxide additive. According to X-ray diffraction data, the parent powders mainly consisted of oxides characteristic of stoichiometric phases: MgO, CaO, and γ-Al_2O_3 (Fig. 1a). Titanium dioxide was a mixture of two phases: rutile and anatase. The structure of the decomposition product of lanthanum nitrate was similar to the structure of $La(OH)_3$ [6]; this is likely due to hydrolysis of the salt on storage in air. In all cases, premixed powders containing 20 wt % oxide additives were subjected to hydrothermal treatment at 200°C and then calcined at 540°C as described elsewhere [6].

The techniques used for studying particle size distributions, phase compositions, dopant concentrations in cermets, and macrotextures, as well as methods for the determination of total pore volumes and for microtextural analysis based on the adsorption–desorption isotherms of nitrogen and argon, were described previously [1–4, 7, 8]. The concentrations of an aluminum oxide phase in Al_2O_3/Al matrices were determined by gravimetric and X-ray diffraction analysis (from ratios between the integrated intensities of 4.4.0 and 2.2.0 peaks for γ-Al_2O_3 and aluminum metal, respectively). A calibration graph was plotted with the use of mechanical mixtures of powdered Al and γ-Al_2O_3 with known ratios between the components. The integrated intensities of diffraction peaks were determined by background subtraction and approximation of experimental peaks with Lorentz functions with the use of the ORIGIN 5.0 program. The amounts of oxide dopants in the resulting composites were determined from chemical analysis data obtained by atomic absorption spectrophotometry.

RESULTS AND DISCUSSION

1. Composition and Macroscopic Characteristics of Composites (Basic Relationships)

1.1. Phase composition of composites. The X-ray diffraction patterns of all the tested cermet samples

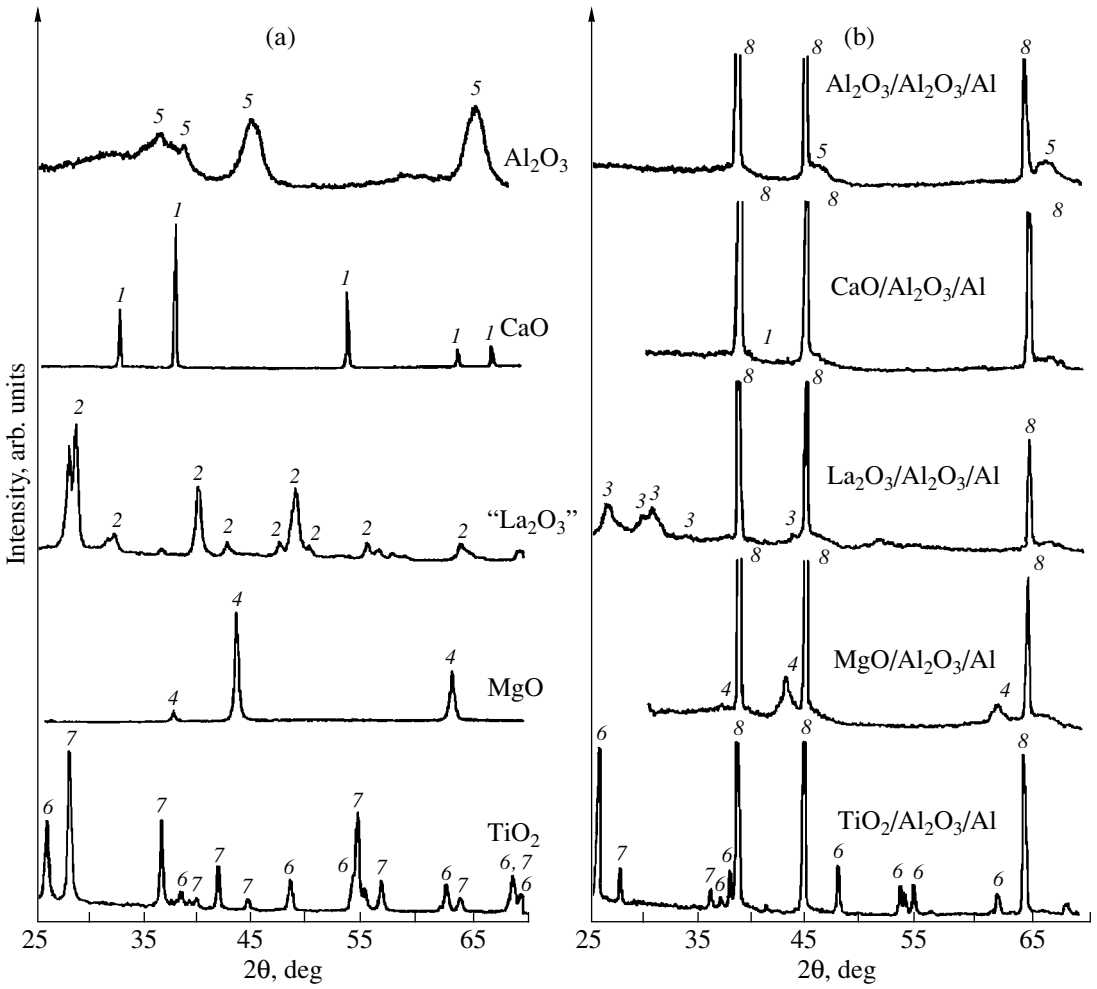

Fig. 1. Diffraction patterns of (a) powdered oxides and (b) $MO_x/Al_2O_3/Al$ composites obtained after mixing oxide dopants with aluminum powder, hydrothermal treatment, and calcination. Reflections due to various phases are numbered as follows: (*1*) CaO, (*2*) $La(OH)_3$, (*3*) "La_2O_3," (*4*) MgO, (*5*) γ-Al_2O_3, (*6*) anatase, (*7*) rutile, and (*8*) Al^0.

exhibited peaks at 111, 200, and 220 corresponding to aluminum metal and weak broad peaks (200 and 440) corresponding to cubic spinel (γ-Al_2O_3) (Fig. 1b). The intensity of these peaks was higher in a composite with an Al_2O_3 dopant. In a sample of $TiO_2/Al_2O_3/Al$, anatase and rutile phases were retained; however, the relative intensity of the anatase phase increased (cf. Figs. 1a and 1b). The diffraction pattern of an $MgO/Al_2O_3/Al$ composite exhibited broad peaks corresponding to interplanar distances of 2.44, 2.10, and 1.49 Å, which are characteristic of MgO [9]. An $La_2O_3/Al_2O_3/Al$ composite exhibited broadened diffraction peaks corresponding to interplanar distances of 3.36, 3.03, and 2.94 Å, which are characteristic of a defect hexagonal phase of La_2O_3 [10] with great changes in the lattice parameters ("La_2O_3" is the initial La-containing additive). A CaO-containing composite exhibited no lines due to oxide (CaO) and hydroxide ($Ca(OH)_2$) phases [11] to within the experimental error of X-ray diffraction analysis. Thus, powdered additives underwent a number of transformations as a result of hydrothermal treatment and thermal decomposition in air. However, a set of simple phases of MO_x oxides, Al_2O_3, and aluminum metal was predominant in the resulting composites (except for CaO). Of course, it is impossible to exclude completely the formation of mixed oxides like solid solutions. However, their fraction is low because the products of the interaction of MO_x and Al_2O_3 were not detected in noticeable amounts. This simplifies the subsequent calculations because, to a first approximation, we can consider the tested composites as mechanical mixtures of oxides and residual aluminum metal.

1.2. Evaluation of the degree of aluminum conversion from the analysis of the resulting composites. It is well known that the synthesis of porous composites based on an Al_2O_3/Al matrix includes treatment under hydrothermal conditions and thermal treatment in air [1–3]. At the first stage, aluminum is oxidized to form hydrated products. The hydration of oxide dopants added can also occur. At the second stage, the

hydration products are decomposed without the subsequent oxidation of aluminum in air. The conversion of aluminum (α) into aluminum oxide is [1]

$$\alpha = \frac{y}{1 + X_0(1 - y)}, \quad (1)$$

where $X_0 = (m^0_{Al_2O_3} - m^0_{Al})/m^0_{Al_2O_3} = 0.89$ characterizes the relative change of weight upon the complete conversion of aluminum into an oxide, and it is a characteristic value of the given reaction [1].

However, for Al_2O_3/Al with oxide additives, the relationship between the composition of the resulting composite and the conversion of aluminum was more complicated. Moreover, the surface of the composite particles was completely covered with water under hydrothermal conditions at the equilibrium pressure of water vapor. Therefore, hydrated products can be partially dissolved, and the dissolved products can react with a protective oxide layer and, consequently, can considerably affect the process of oxidation of aluminum with oxide additives [3]. Thus, the degree of aluminum conversion in the presence of oxides can be changed as compared with pure aluminum powder. Substance removal from a mold into the mother liquor of an autoclave can present additional problems. As mentioned above, the chemical and phase composition of an oxide dopant can also be affected. In all of these cases, the conversion of aluminum should be evaluated in different manners.

Let us consider the simplest case when the entire increase in the weight of a powder after hydrothermal treatment and calcination was due to the formation of aluminum oxide and the weight of dopants after the above transformations was approximately equal to the weight before the hydrothermal treatment. The weight fraction of a dopant in the resulting composite is designated as z, the fraction of Al_2O_3 formed from aluminum metal is designated as y', and the fraction of unreacted aluminum metal is designated as x. These weight fractions are related by the following balanced equation for the resulting composite:

$$x + y' + z = 1. \quad (2)$$

Note that previously [1], the fraction of the oxide in an Al_2O_3/Al matrix was designated as y:

$$y = \frac{m_{Al_2O_3}}{m_{Al_2O_3} + m_{Al}}. \quad (3)$$

Expressing the weight of aluminum oxide produced from aluminum ($m_{Al_2O_3}$) and the weight of residual aluminum in the MO_x/Al_2O_3/Al composite in terms of the total weight of the composite (m_0) and the weight of the oxide (m_{MO_x}) and normalizing to m_0, we obtain

$$y = \frac{m_{Al_2O_3}}{m_0 - m_{MO_x}} = \frac{y'}{1 - z}. \quad (4)$$

Substituting (4) in Eq. (1) gives the following relationship between the composition of the MO_x/Al_2O_3/Al composite and the conversion of aluminum:

$$\alpha = \frac{y'}{1 - z + X_0(1 - z - y')}. \quad (5)$$

The value of z was determined from the results of chemical analysis with consideration for the stoichiometry of the corresponding oxides supported by X-ray diffraction data; the value of y' was calculated based on gravimetric data.

Let us analyze how the value of z depends on the initial oxide content of a powder mixture and on the conversion of aluminum. For an initial aluminum powder without oxide additives, the weight of metal ceramics is calculated as follows [1]:

$$m_\alpha = m^0_{Al}(\alpha X_0 + 1). \quad (6)$$

The weight of a composite (m_0) containing a dopant is related to the total weight of the initial powder mixture (m^0) and to the fraction of the oxide dopant (z') in accordance with the following expression:

$$m_0 = m^0(\alpha X_0 + 1)(1 - z') + m^0 z'. \quad (7)$$

The fraction of the dopant in the composite is calculated from the following equation, which includes the values of X_0, z', and m_0 and the conversion of aluminum:

$$z = \frac{z' m^0}{m_0} = \frac{z'}{1 + \alpha X_0(1 - z')}. \quad (8)$$

The calculated and experimental values of z for samples containing Al_2O_3, MgO, and TiO_2 are consistent (Table 1). Consequently, it is believed that substance removal from a mold is insignificant in the case of these composites, and the value of α can be evaluated by gravimetry.

The experimental value of z was found much lower than the calculated value for a calcium-containing composite. Therefore, in this case the calculation of the degree of conversion from gravimetric data is impossible because substance removal from a mold is considerable. The experimentally found concentration of a lanthanum oxide additive in the resulting product was also noticeably lower than the calculated value; this can be due to the hydroxide $\longrightarrow$ oxide phase transition, which was noted previously. As a result, the concentration of stoichiometric lanthanum oxide in the initial powder mixture was ~17% in place of the calculated 20%. Both processes resulted in underestimated values of α. Indeed, an independent estimation of the degrees of aluminum conversion from X-ray diffraction data with the use of Eq. (4) for Ca- and La-containing materials demonstrated that they exhibited somewhat higher

Table 1. Characteristics of $MO_x/Al_2O_3/Al$ composites

Parameter	MO_x					
	–	CaO	La_2O_3	MgO	Al_2O_3	TiO_2
α	0.11	0.22 (0.27)**	0.13 (0.24)**	0.32	0.18	0.06
d, μm	24.0	9.2	13.1	21.9	7.7	8.4
z	–	0.03	0.12	0.15	0.18	0.19
z*	–	0.17 (0.17)**	0.18 (0.15)**	0.16	0.18	0.19
δ_0, g/cm^3	1.19	1.05	1.09	0.80	1.07	1.01
δ'_α, g/cm^3	1.31	1.24 (1.10)**	1.19 (1.28)**	0.97	1.19	1.05
δ_α, g/cm^3	1.34	1.34	1.40	1.31	1.38	1.03
f_v	0.98	0.86 (0.82)**	0.85 (0.91)**	0.81	0.88	1.02
y'	0.19	0.40	0.33	0.40	0.24	0.10
ρ_{MO_x}, g/cm^3	–	2.42	4.52	3.29	3.30	4.04
V_α^{***}, cm^3/g	0.40	0.54** (0.37)	0.45	0.71 (0.51)	0.49 (0.39)	0.61
ρ_α, g/cm^3	2.79	2.74	3.20	3.05	2.83	2.99
V_α, cm^3/g	0.39	0.38	0.40	0.44	0.37	0.64
ε'	0.57	0.60	0.66	0.72	0.62	0.66
ε	0.52	0.51	0.56	0.57	0.51	0.66
Π, MPa	9.8	4.0	1.0	0.6	3.8	0.2

Note: α is the conversion of aluminum; d is the average particle size; δ_0 is the packed density of powders; z is the concentration of MO_x in the composite, as calculated from chemical analysis data; δ'_α is the apparent density of composites (calculated); δ_α is the apparent density of composites (experimental); f_v is the shrinkage factor ($\delta'_\alpha/\delta_\alpha$); y' is the fraction in the composite of aluminum oxide produced from aluminum after the hydrothermal treatment and calcination of powders; ρ_{MO_x} is the true density of a powdered dopant; V_α^{***} is the specific pore volume calculated from Eq. (16); ρ_α is the apparent density of composites; V_α is the specific pore volume calculated from the true and apparent densities of composites; ε is the porosity of the composite; ε' is the porosity of charge; Π is the crushing strength.

* Calculations from gravimetric data were performed using Eq. (8).

** Calculations from X-ray diffraction data were performed.

*** Pore volumes with consideration for shrinkage factors are given in parentheses.

values (Table 1). However, in this case, the values of z only approached experimental values for the lanthanum-containing composite (Table 1). For the calcium-containing sample, the values of z differed by a factor of almost 6. Moreover, an estimation of the possible concentration of an additive at 100% aluminum conversion demonstrated that the value of z cannot be lower than 12%. The main reason for this discrepancy in the case of the composite with a CaO additive consists of an assumption regarding the constancy of the oxide content (the absence of removal), that is, on the constancy of the value of z', which was used in Eq. (8), as well as in Eq. (5), in implicit form. The simultaneous occurrence of two processes, one of which increases the weight of the powder, whereas the other decreases this weight, did not allow us to predict the weight of the composite as a whole based on only the kinetic data on possible conversions of aluminum.

However, the effective concentration of a calcium oxide additive can be determined based on the assumption that the removal of the dopant and the oxidation of aluminum are independent processes. In this case, the value of z' can be evaluated after the completion of the stage of calcium oxide removal with the use of Eq. (8). We found that, with the use of the values of α and z obtained independently, the calcium oxide content of the starting mixture should be no higher than 4%.

The results summarized in Table 1 allowed us to conclude that, indeed, oxide dopants introduced into an Al_2O_3/Al matrix considerably increase the reactivity in almost all cases. Higher values of aluminum conversion are typical of alkaline-earth metal oxide additives, which are more soluble in water; it is likely that they are favorable for the more rapid loosening of the protective layer on the surface of aluminum. More amphoteric oxides of lanthanum and aluminum have less pronounced effects on the reactivity of aluminum (Table 1). A decrease in the conversion of aluminum in the presence of titanium oxide can be due to an inhibiting effect of titanium compounds on the oxidation process [12].

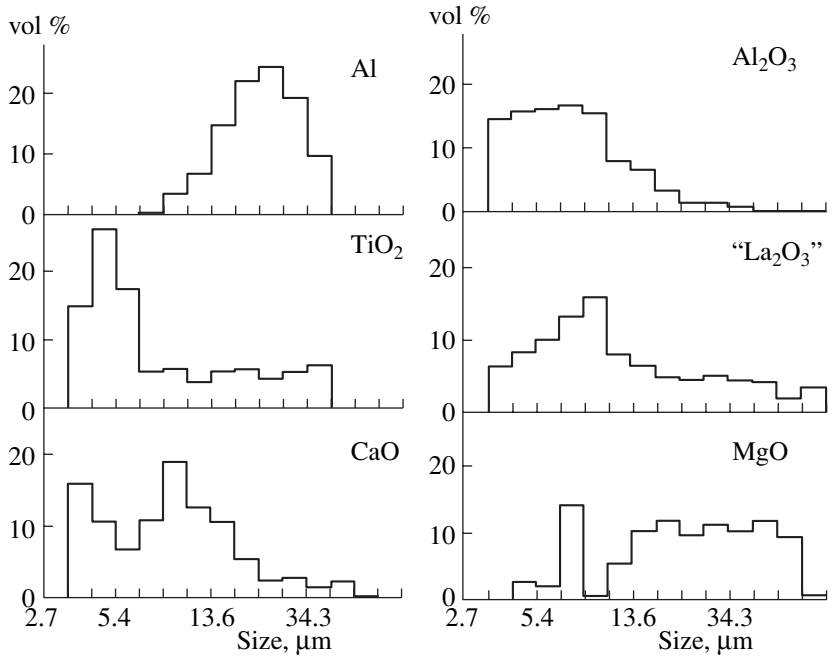

Fig. 2. Particle-size distribution of powders used for the synthesis of MO_x/Al_2O_3/Al composites.

1.3. Dependence of the apparent density of metal ceramics on the packed density of powder. The porosity can either increase (i.e., the packed density decreases) or decrease upon mixing two powdered substances. The packed density depends on the amount of an oxide added and on the ratio between the average particle size of the additive and of the parent aluminum powder [13]. The density of a powder mixture is lower than the packed density of the parent aluminum powder (δ_0) (Table 1) even when the average particle size is noticeably greater (Fig. 2). This could be due to the predominant distribution of oxide particles in contact sites between aluminum particles rather than in natural cavities formed by aluminum particles because of the particle-size anisotropy of the powder added and surface roughness [13], as supported by scanning electron microscopy (Fig. 3). Electrostatic interactions between particles can also occur to prevent the powder particles from more closely packing in the course of charging.

The apparent density of the resulting granulated composites (δ'_α) is equal to [1]

$$\delta'_\alpha = \frac{m_0}{V_0} = \frac{m_\alpha + m_{MO_x}}{V_0}, \quad (9)$$

where V_0 = const is the volume of the mold (the volume of the resulting granulated composite), and m_α is the weight of an Al_2O_3/Al matrix at the given degree of aluminum conversion. In the starting mixture of powdered aluminum with an oxide dopant (of weight $m^0 = m^0_{Al} + m^0_{MO_x}$), the weight of the oxide dopant is $m^0_{MO_x} = m^0 z'$, where z' is the weight fraction of MO_x in the mixture, and the weight of aluminum is $m^0_{Al} = m^0(1 - z')$. Taking into account Eq. (6) and assuming that the weight of the oxide remained almost unchanged after hydrothermal treatment and calcination ($m^0_{MO_x} \approx m_{MO_x}$), we obtain the following expression for the apparent density of the resulting composites:

$$\delta'_\alpha = \delta_0[1 + \alpha X_0(1 - z')]. \quad (10)$$

At $z' = 0$, Eq. (10) is converted into an equation [1] for the apparent density of composites without additives. The value of δ_0 in Eq. (10) characterizes the density of the initial powder containing aluminum and an oxide dopant, whose concentration is equal to z'.

Equation (10) was used for evaluating the apparent densities of cermet samples containing the oxides of titanium, aluminum, magnesium, and lanthanum. For lanthanum oxide, the degree of conversion calculated from X-ray diffraction data and a corrected value of z' were used. According to data given in Table 1, the experimentally found apparent densities of the resulting composites were higher. Experimental errors in the gravimetric determination of an increase in weight can be as high as ±10% because of the possibility of partial losses of aluminum powder in the course of loading, and losses of the composite in the course of discharging from the mold. Therefore, the calculated apparent densities are consistent with experimental data. However, this discrepancy can also be explained by the shrinkage

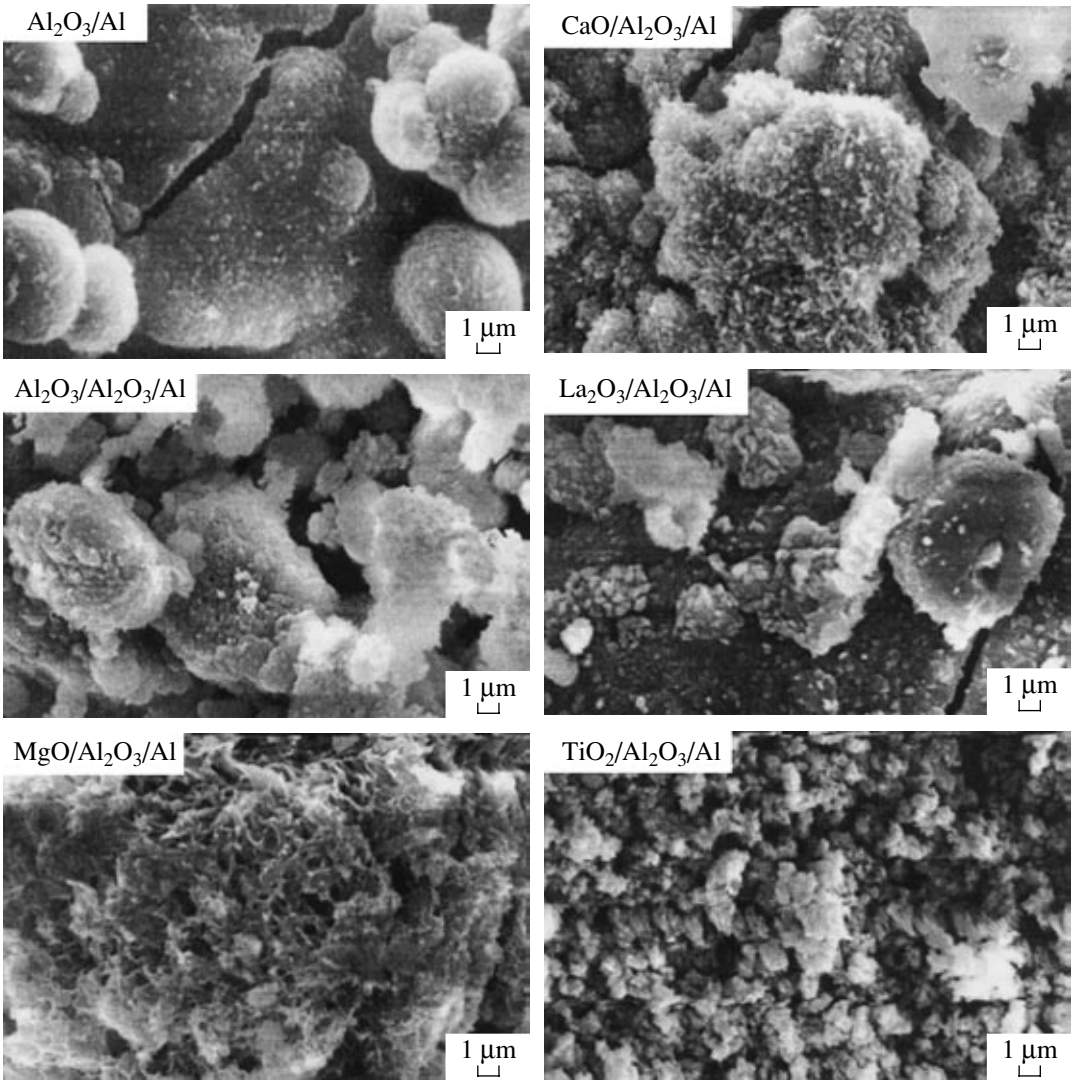

Fig. 3. Electron micrographs of $MO_x/Al_2O_3/Al$ composites.

of composite granules after calcination [1]. The shrinkage factor can be calculated from the equation

$$f_v = \frac{V_f}{V_0} = \frac{\delta'_\alpha}{\delta_\alpha}, \quad (11)$$

where δ'_α is the apparent density of granules without shrinkage (calculated), and δ_α is the apparent density of granules with consideration for shrinkage. With consideration for this shrinkage factor, the accuracy of the estimation of apparent densities can be significantly improved (Table 1).

Note that Eq. (10) cannot be used if the removal of the substance from the mold is considerable because the packed density of the initial powder changes. However, the relationship between the apparent density of the composite and the conversion of aluminum can also be expressed analytically in this case, taking into account the actual concentration of an additive in the mixture. With the use of Eqs. (2) and (6), we can express a relationship between the weight of the composite (m_0) and the weight of the Al_2O_3/Al matrix (m_α) formed upon the incomplete oxidation of aluminum as follows:

$$m_0 = \frac{m_\alpha}{1-z} = \frac{m^0_{Al}(1+\alpha X_0)}{1-z}. \quad (12)$$

In turn, $m^0_{Al} = m^0(1-z')$ and

$$\delta_\alpha = \frac{m_0}{V_0} = \delta_0\frac{(1-z')(1+\alpha X_0)}{1-z}. \quad (13)$$

In this case, the dependence of changes in z on the conditions of the hydrothermal synthesis, the nature of oxide dopants, and the design features of the mold should be studied in order to predict the pore volume.

According to X-ray diffraction and chemical analysis data, the apparent density of a $CaO/Al_2O_3/Al$ composite was lower than that without consideration for losses (Table 1), whereas the shrinkage factor increased, which can be explained by a decrease in the substance weight per unit volume. It is likely that, at a low dopant concentration (20%), the Al_2O_3/Al matrix formed in the course of hydrothermal treatment exerted the strongest effect on the properties of composites. The effect of the oxide dopant manifested itself in changes in the reactivity of aluminum and, consequently, in the composition of the Al_2O_3/Al matrix.

1.4. Dependence of the pore volume of $MO_x/Al_2O_3/Al$ composites on the conversion of aluminum and on the amount of an oxide dopant. The total pore volume in a composite can be calculated from the true density (ρ'_α) and the apparent density of granules (δ'_α). With consideration for the balanced relationship (2), we obtain

$$V_\alpha = \frac{1}{\delta'_\alpha} - \frac{1}{\rho'_\alpha} = \frac{1}{\delta'_\alpha} - \frac{x}{\rho_{Al}} - \frac{y'}{\rho_{Al_2O_3}} - \frac{z}{\rho_{MO_x}}. \quad (14)$$

The total pore volume of $MO_x/Al_2O_3/Al$ composites is

$$V_\alpha = \frac{1}{\delta_0[1+\alpha X_0(1-z')]} - \frac{(1-\alpha)(1-z')}{\rho_{Al}[1+\alpha X_0(1-z')]} - \frac{\alpha(X_0+1)(1-z')}{\rho_{Al_2O_3}[1+\alpha X_0(1-z')]} - \frac{z'}{\rho_{MO_x}[1+\alpha X_0(1-z')]}. \quad (15)$$

The first three terms of Eq. (15), which depend on the true densities of components and on the conversion of aluminum, make the main contribution to the specific pore volume. In our case, we assumed that the density of aluminum oxide formed in the oxidation of aluminum metal is equal to the density of the oxide in pure Al_2O_3/Al synthesized under the same conditions at similar values of α (2.92 g/cm^3) [1]. According to X-ray diffraction data (Fig. 1), TiO_2 and "La_2O_3," which is actually a hydroxo compound, underwent noticeable changes in the phase composition after hydrothermal treatment and calcination. In this case, it is evident that the true densities of these dopants changed, and this change could affect both the calculated pore volumes and the apparent densities of granules, which were calculated previously. However, even at 100% conversion of rutile into anatase, a maximum change in the volume of titanium dioxide would be ~0.05 g/cm^3 with consideration for the difference between the true densities (4.2–4.3 g/cm^3 for rutile and 3.6–3.95 g/cm^3 for anatase [14, 15]), whereas it would be no higher than 0.006 g/cm^3 at a TiO_2 concentration of ~20% in the composite. This corresponds to a measurement error of ~1.6%.

A comparison of data calculated from the above equations with experimental data on the apparent and true densities of granules provides support for the assumptions made in the calculations (Table 1). The exception was provided by a magnesium-containing sample, which was significantly different from the others even at the stage of loading the initial powders because magnesium oxide is very loose (Table 1). The composite with an Al_2O_3 additive exhibited a small but noticeable discrepancy between experimental and calculated densities. Internal porosity and, consequently, the greatest shrinkage factors are characteristic of aluminum oxide, as well as of MgO (Table 1). Taking into account shrinkage (the replacement of 1 with f_v in the first term of Eq. (15)) for these samples gave a satisfactory agreement between calculated and experimental data. The discrepancy between calculated and experimental data can be explained by the formation of closed pores on calcination; these pores are inaccessible to helium molecules.

Note that, although the packing of the initial powders was looser, the pore volume of $MO_x/Al_2O_3/Al$ composites changed insignificantly as compared with the matrix of Al_2O_3/Al (Table 1). This was likely due to a compensating effect of a higher degree of conversion of aluminum with dopants, as compared to that of pure aluminum. The exception was provided by a composite with TiO_2 as a result of a low degree of conversion (Table 1). It is likely that, at low concentrations of oxide dopants, the process of hydroxide (oxide) formation has a crucial effect on the texture properties of complex composites.

To evaluate the pore volume of a $CaO/Al_2O_3/Al$ composite, Eq. (14) was rearranged to take into account Eqs. (12) and (13). This allowed us to calculate pore volumes for the case of substance removal from the mold using the values of z, z', and α, which was calculated from X-ray diffraction data, by the following equation:

$$V_\alpha = \frac{f_v(1-z)}{\delta_0(1-z')(1+\alpha X_0)} - \frac{(1-\alpha)(1-z')}{\rho_{Al}[1+\alpha X_0(1-z')]} - \frac{\alpha(X_0+1)(1-z)}{\rho_{Al_2O_3}(1+\alpha X_0)} - \frac{z'}{\rho_{MO_x}[1+\alpha X_0(1-z')]}. \quad (16)$$

The first three terms of Eq. (16), which depend on the true densities of components and on the conversion of aluminum, make the main contribution to the value of V_α. Equation (16) was derived based on the assumption that calcium oxide and alumina occurred individually in the composite without the formation of aluminocalcium spinel. Taking into account that the contribution of the last term of the equation is small, we believe that this assumption has an insignificant effect on the total pore volume. Moreover, the shrinkage factor was taken into consideration (see Table 2). Thus, the equations derived allowed us to evaluate pore volumes for dopants that are sparingly soluble or soluble under hydrothermal conditions. The data estimated above also suggest that the shrinkage of granulated composites should be necessarily taken into account for oxides with very loose packing and developed intrinsic poros-

Table 2. Microtexture characteristics of $MO_x/Al_2O_3/Al$ composites found from an analysis of nitrogen and argon adsorption–desorption isotherms

Sample	S_α, m^2/g (Ar)		Texture characteristics of composites (N_2)					
	MO	total composite, calculated	pore volume, cm^3/g		specific surface area, m^2/g			h, Å
			$V_\alpha + V_\mu$	V_{ox}	S_Σ	S_{outer}	S_{ox}	
–	–	–	0.0269	–	31.5	2.9	–	19
CaO	0.2	51	0.0411	0.10	40.3	13.9	94	31
"La_2O_3"	4.4	29	0.0453	0.10	64.9	22.9	141	22
MgO	26	64	0.0708	0.13	110.4	60.7	201	29
Al_2O_3	220	76	0.0464	0.11	88.2	62	210	35
TiO_2	8.2	26	0.0144	0.05	29.9	18.1	103	24

Note: $V_\alpha + V_\mu$ is the specific pore volume within aggregates; S_Σ is the total specific surface area of composites found from a comparative analysis of nitrogen adsorption isotherms; S_{outer} is the outer surface area of aggregates; $S_{ox} = \frac{S_\Sigma}{z + y'}$; $V_{ox} = \frac{V_\alpha + V_\mu}{z + y'}$; S_α (calculated) is the specific surface area calculated on the assumption that the properties of Al_2O_3 and MO_x are additive; h is the average pore size from a comparative analysis of nitrogen adsorption isotherms.

ity and in the case of considerable substance losses from the mold.

1.5. Porosity and mechanical strength of composites. Among the factors responsible for the mechanical strength of a porous solid prepared from powders, the strength of a single contact between particles and the total porosity of the material related to the number of contacts between particles can be pointed out [16]. Because a primary contact between particles appears even at the stage of mixing powders, we estimate the total porosity (ε') based on concepts [16] as follows:

$$\varepsilon' = 1 - \frac{1}{V_0}\left(\frac{m_{MO_x}}{\rho_{MO_x}} - \frac{m^0_{Al}}{\rho_{Al}}\right) = 1 - \frac{m^0}{V_0}\left(\frac{z'}{\rho_{MO_x}} - \frac{1-z'}{\rho_{Al}}\right) = 1 - \delta_0\left(\frac{z'}{\rho_{MO_x}} - \frac{1-z'}{\rho_{Al}}\right). \quad (17)$$

All the designations are analogous to those given above. Table 2 summarizes the values of porosity for $z' = 0.2$. As expected, the porosity of powders increased on the addition of dopants. This produces objective prerequisites for a decrease in the mechanical strength of subsequently formed granules even at the stage of loading, at least in powders obtained in this study.

The porosity of composites was evaluated from the following published equation [1]:

$$\varepsilon = \frac{\rho_\alpha V_\alpha}{1 + \rho_\alpha V_\alpha}. \quad (18)$$

Data given in Table 2 indicate that, in the course of formation of composites, the porosity decreased (as compared with the parent mixture) because of an increase in the volume of the solid and partially because of the shrinkage of granules. In this case, the difference between the porosities of the pure "Al_2O_3/Al" matrix and an oxide-doped composite was insignificant. On the other hand, the mechanical strength of composites decreased stepwise on the addition of oxides (Table 2). It is believed that the addition of powdered oxides dramatically decreases the number of contacts between aluminum particles, which are covered with a layer of porous alumina, in the composite (Fig. 3) [17]. The strength of contacts between oxide dopant and Al_2O_3/Al particles is much lower. This results in a dramatic decrease in the mechanical strength of complex composite granules. At the same time, the trend has been toward a decrease in the porosity and mechanical strength of granules on the addition of oxide dopants. As a first approximation, we attempted to perform linearization using the following empirical equation proposed by Bal'shin [18]:

$$\Pi = \Pi_0(1 - \varepsilon)^m, \quad (19)$$

where m is the ratio of the total weight of the material to the weight of the material that assumed a load under the action of a force. We estimated the value of m from data given in Table 2 and found that this value is much higher (~8) than that for simple Al_2O_3/Al composites (~2) [1]. It is likely that the absolute value of m was inadequately determined for complex composites because the number of experimental points was small. However, undoubtedly the general trend is for decreasing the parameter m on going from simple composites to more complex cermets.

Because correlation Eq. (19) is usually applied to samples of the same composition, it is believed that powdered oxide dopants indirectly affect (as an "inert" material) the mechanical strength of composites. In this case, the total weight of the composite, which is responsible for its strength, significantly decreases. Conse-

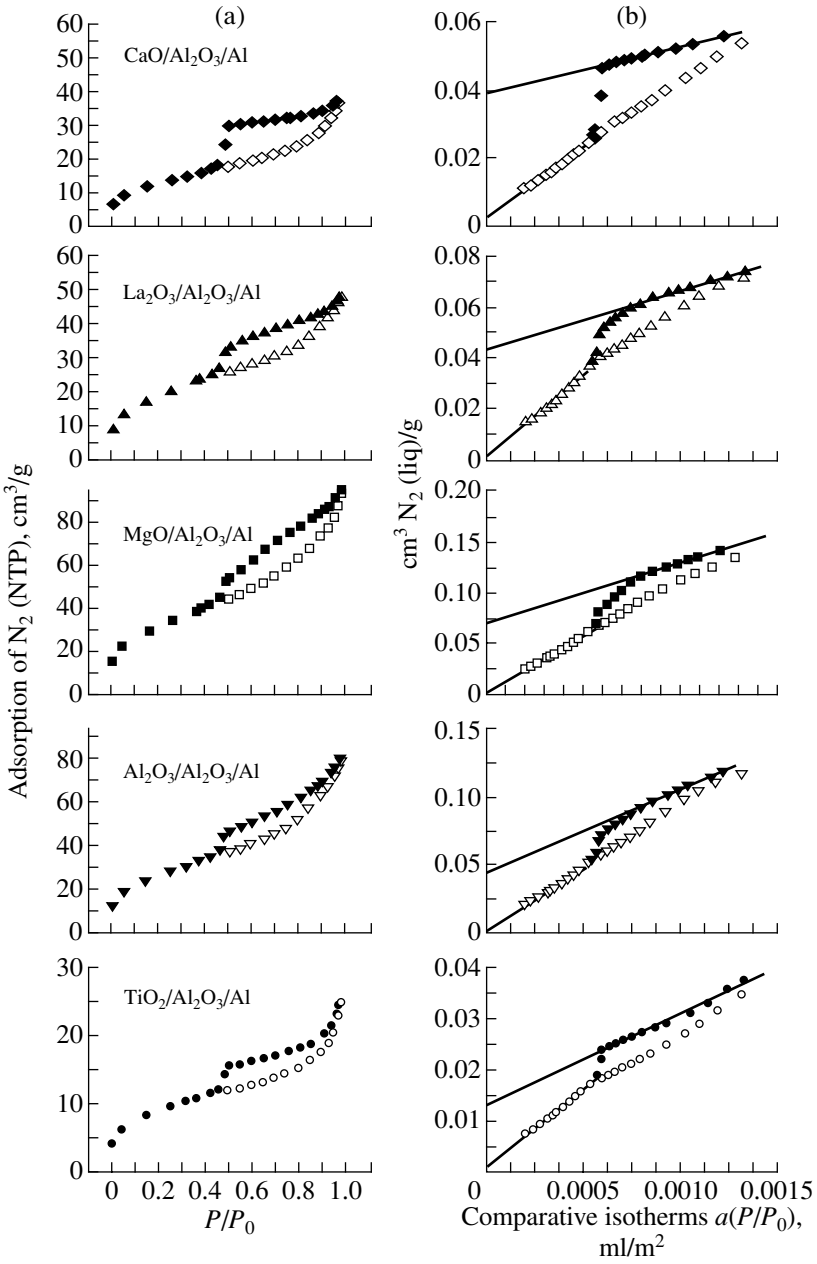

Fig. 4. Isotherms of nitrogen adsorption–desorption at 77 K for $MO_x/Al_2O_3/Al$ composites: (a) primary data and (b) comparative forms.

quently the deciding factor responsible for the strength of granules, independent of the nature of the dopant, is the total number of contacts between "Al_2O_3/Al" and "Al_2O_3/Al" particles in the matrix of Al_2O_3/Al.

2. Composition and Microtexture of Composites

2.1. Micropore and mesopore structures of composites. All the isotherms of composites with low-porosity oxide additives (CaO, "La_2O_3," and TiO_2), which are shown in Fig. 4a, are characteristic of ordered high-porosity aggregates with a developed network of mutually intersecting pores [2, 6]. According to the IUPAC classification [19], they belong to the H2 type with respect to the shape of a hysteresis loop; they are similar to the isotherms that correspond to an Al_2O_3/Al matrix [2] and differ only in the value of adsorption. This provides support for the above hypothesis that the micropore and mesopore structures of $MO_x/Al_2O_3/Al$ composites primarily depend on the texture of alumina formed by the oxidation of aluminum powder, whereas the dopants only modified the properties of this oxide.

At the same time for high-porosity additives (MgO and Al_2O_3) (Fig. 4a), the isotherms approached the H3

type, which is characteristic of slitlike pores [19]. For a composite with powdered alumina added, a very narrow pore-size distribution was observed, which is not typical of ordinary γ-Al_2O_3 [20].

The pore structure was described in detail based on the analysis and comparison of the shapes of adsorption–desorption curves (Fig. 4b). This method is based on a comparison of experimental curves with a standard adsorption isotherm obtained on a nonporous sample [21]. The outer surface area S_{outer} of oxide particle aggregates of composites [2] was evaluated from the slope of the linearized desorption branch of an isotherm. The extrapolation of this portion of a straight line to the ordinate axis allowed us to determine the total micropore and mesopore volume V_a within aggregates. After the extrapolation of the linearized adsorption branch of a plot to the ordinate axis, we calculated the volume of ultramicropores V_μ with molecular sizes, and the total specific surface area S_Σ of composites was calculated from the slope of the straight line. The average width of micropores and mesopores was found from the following equation for slitlike pores:

$$h = 2V_a/(S_\Sigma - S_{outer}). \quad (20)$$

Note that the outer surface area of samples containing oxides (~14–60 m^2/g) considerably increased as compared with that of the matrix of Al_2O_3/Al (~3 m^2/g). For MgO and Al_2O_3, this was likely due to the effect of the textures of powder dopants. For the other samples, this was more likely due to the fact that dopant particles prevented the aggregation of the primary particles of aluminum oxides (hydroxides) at the step of their formation as well-crystallized aggregates. The ultramicropore and mesopore volumes of composite samples with low-porosity dopants (except for TiO_2) noticeably increased (by a factor of 2–4) (Table 2). It is likely that oxide dopants, which were partially dissolved in water condensed on the surface of particles, were introduced between the planes of the layered structure of aluminum hydroxide to facilitate the development of its micropore and mesopore structures. The average pore size changed to a lesser extent; therefore, we can conclude that the addition of oxide dopants is favorable for a decrease in the average size of primary alumina particles.

2.2. Nonadditivity of specific surface areas. The specific surface area of a multicomponent system (S_α) with a pronounced interface depends on the concentrations and intrinsic specific surface areas of these components:

$$S_\alpha = xS_{Al} + y'S_{Al_2O_3} + zS_{MO_x}. \quad (21)$$

Because oxide dopants affect the reactivity of aluminum, the alumina content of composites and the conversion of aluminum change. As found previously [2], $S_{Al_2O_3}$ is also not a constant value, and it decreases from ~250 m^2/g at $\alpha = 0.05$ to ~150 m^2/g in the range of $\alpha =$ 0.06–0.25. Therefore, we chose $S_{Al_2O_3} = 250$ m^2/g for a composite containing TiO_2 and a value of 150 m^2/g for the other samples. Table 3 summarizes experimental values (S_Σ), as well as the results of the calculations of S_α on the assumption that encapsulation has no effect on the specific surface area of dopants.

As can be seen in Table 3, except for a sample with CaO, the specific surface areas of composites calculated on the assumption that properties are additive are lower than experimental values. This provides support for the hypothesis on the additional dispersion of hydroxide (oxide) components. It is most likely that the products of hydrolysis and partial dissolution of MO_x affect the process of aging of the hydroxo compounds of aluminum as well as the particle size, structure, and aggregation of hydroxo poly compounds [22, 23], to change the texture of the resulting aluminum oxide. This is also evident from a dramatic change in the surface macrorelief of a composite (according to scanning electron microscopic data) as compared with an Al_2O_3/Al matrix (Fig. 3). Flaky aggregates are typical of composites with MgO, whereas clotted aggregates are characteristic of La_2O_3 and TiO_2. Needle-shaped aggregates are formed in composites with calcium oxide; this can be due to the formation of calcium aluminates.

An inverse effect of hydrothermal treatment and an aluminum hydroxide matrix on the nonadditive dispersion of dopants can also occur. Calcium oxide, which remained in the mold after washing, can remain on the surface of Al_2O_3 as clusters; lanthanum hydroxide was converted into an oxide; magnesium oxide and aluminum oxide did not undergo such noticeable transformations. In general, it is believed that the synergism of properties, which manifests itself in the dispersion of composite particles, is typical of the test samples of metal ceramics to some extent.

It is likely that the main effect of oxide dopants on the properties of composites consists in the dispersion of alumina particles. We estimated $S_{Al_2O_3}$ from Eq. (20) on the assumption that the specific surface area of MO_x remained almost unchanged; this value was ~200 or ~440 m^2/g for a composite with CaO or La_2O_3, respectively. This makes it possible to additionally control the texture of the resulting Al_2O_3.

In general, based on the experimental results and calculated data, we can conclude that complex physicochemical processes occur in the course of encapsulation of powdered oxides in an Al_2O_3/Al matrix. These physicochemical processes facilitate the appearance of nonadditive properties of the resulting composites as compared to their individual components. Even at the stage of loading powders, the introduction of oxide dopants increased the porosity of the mixture (at least in the materials tested). The hydrolysis or partial dissolution of oxides accompanied by substance removal from the mold into the mother liquor of an autoclave can occur under hydrothermal conditions to considerably decrease the concentration of a dopant (such as CaO). A combination of hydrothermal treatment with

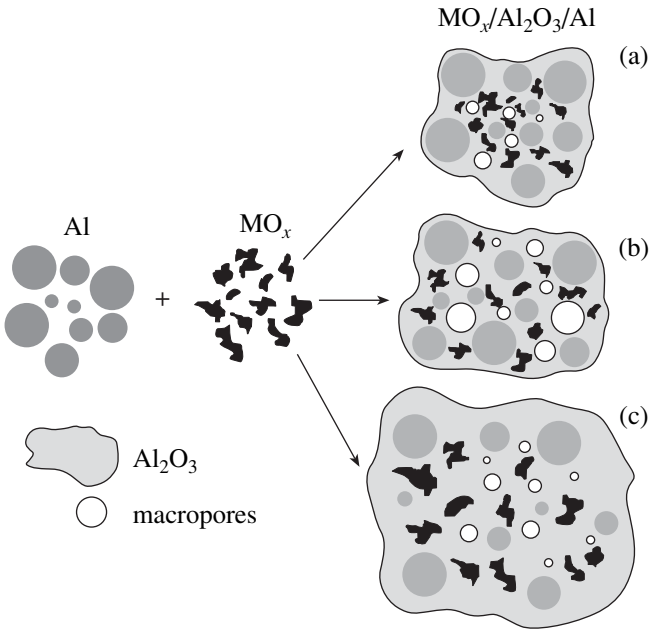

Fig. 5. Schematic diagram of the formation of the macrotexture of $MO_x/Al_2O_3/Al$ composites: (a) a packing of powders without changes in the conversion of aluminum, (b) a looser packing of powders without changes in the conversion of aluminum, and (c) a looser packing of powders with an increase in the conversion of aluminum.

calcination can facilitate the thermal decomposition of a hydroxide to an oxide (La_2O_3). Dopants considerably affect the oxidation of aluminum and hence the concentration of Al_2O_3 in the composite; they also affect the nonadditive texture properties of composites to facilitate the dispersion of alumina particles. High-porosity oxide dopants such as MgO and Al_2O_3 can exert a direct effect on the texture of $MO_x/Al_2O_3/Al$ composites.

Figure 5 schematically shows the formation of the macrotexture of $MO_x/Al_2O_3/Al$ composites. Scheme a illustrates the case of a denser packing of powders as compared with the initial aluminum, whereas scheme b shows a looser packing, which is favorable for an increase in the macropore volume of the composite. In this case, the conversion of aluminum remained approximately constant in versions a and b. Scheme c occurred in our case, according to which a looser packing was compensated by a higher conversion of aluminum. As a result, only the ratio between the volumes of micropores and mesopores localized in an oxide matrix and macropores localized between the particles of a powder mixture was changed.

ACKNOWLEDGMENTS

This work was supported by the Russian Foundation for Basic Research (project nos. 99-03-32853 and 02-03-32277). Yu.V. Potapova acknowledges the support of INTAS (grant no. YFS-00-199).

REFERENCES

1. Tikhov, S.F., Fenelonov, V.B., Sadykov, V.A., Potapova, Yu.V., and Salanov, A.N., *Kinet. Katal.*, 2000, vol. 41, no. 6, p. 907.
2. Tikhov, S.F., Zaikovskii, V.I., Fenelonov, V.B., Potapova, Yu.V., Kolomiichuk, V.N., and Sadykov, V.A., *Kinet. Katal.*, 2000, vol. 41, no. 6, p. 916.
3. Tikhov, S.F., Potapova, Yu.V., Sadykov, V.A., Fenelonov, V.B., Tsybulya, S.V., Salanov, A.N., Ivanov, V.P., and Kolomiichuk, V.N., *Kinet. Katal.*, 2003, vol. 44, no. 2, p. 322.
4. Tikhov, S.F., Sadykov, V.A., Potapova, Yu.V., Salanov, A.N., Kustova, G.N., Litvak, G.S., Zaikovskii, V.I., Tsybulya, S.V., Pavlova, S.N., Ivanova, A.S., Rozovskii, A.Ya., Lin, G.I., Lunin, V.V., Ananyin, V.N., and Belyaev, V.V., *Stud. Surf. Sci. Catal.*, 1998, vol. 118, p. 797.
5. Tikhov, S.F., Potapova, Yu.V., Sadykov, V.A., Salanov, A.N., Tsybulya, S.V., Litvak, G.S., and Melgunva, L.F., *React. Kinet. Catal. Lett.*, 2002, vol. 77, no. 1, p. 267.
6. PC PDF no. 36-1481.
7. Tikhov, S.F., Fenelonov, V.B., Zaikovskii, V.I., Potapova, Yu.V., and Sadykov, V.A., *Micropor. Mesopor. Mater.*, 1999, vol. 33, p. 137.
8. Tikhov, S.F., Salanov, A.N., Palesskaya, Yu.V., Sadykov, V.A., Kustova, G.N., Litvak, G.S., Rudina, N.A., Zaikovskii, V.A., and Tsybulya, S.V., *React. Kinet. Catal. Lett.*, 1998, vol. 64, no. 2, p. 301.
9. PC PDF no. 45-0946.
10. PC PDF no. 05-0602.
11. PC PDF no. 28-0775.
12. Kol'tsova, I.S. and Kolyaida, A.Yu., *Zh. Prikl. Khim.*, 2000, vol. 73, p. 1266.
13. Fenelonov, V.B., *J. Porous Mater.*, 1996, vol. 2, p. 263.
14. Rabinovich, V.A. and Khavin, Z.Ya., *Kratkii khimicheskii spravochnik* (Concise Handbook of Chemistry), Leningrad: Khimiya, 1978.
15. *Spravochnik khimika* (Handbook on Chemistry), Moscow: Khimiya, 1965, vol. 2.
16. Fenelonov, V.B., *Kinet. Katal.*, 1994, vol. 35, no. 5, p. 795.
17. Rebinder, P.A., Margolis, L.Ya., and Shchukin, E.D., *Dokl. Akad. Nauk SSSR*, 1964, vol. 154, no. 3, p. 695.
18. Bal'shin, M.Yu., *Nauchnye osnovy poroshkovoi metallurgii i metallurgii volokna* (Scientific Bases of Powder and Fiber Metallurgy), Moscow: Metallurgiya, 1972.
19. Gregg, S.J. and Sing, K.S.W., *Adsorption, Surface Areas, and Porosity*, New York: Academic, 1982.
20. Buelna, G. and Lin, Y.S., *Micropor. Mesopor. Mater.*, 1999, vol. 30, p. 359.
21. Karnaukhov, A.P., Fenelonov, V.B., and Gavrilov, V.Yu., *Pure Appl. Chem.*, 1989, vol. 61, p. 1913.
22. Ivanova, A.S., Skripchenko, E.V., Moroz, E.M., Litvak, G.S., Kustova, G.N., and Krivoruchko, O.P., *Izv. Sib. Otd. Akad. Nauk SSSR, Ser. Khim. Nauk.*, 1989, no. 6, p. 116.
23. Krivoruchko, O.P., Zolotovskii, B.P., Plyasova, L.M., Buyanov, R.A., and Zaikovskii, V.I., *React. Kinet. Catal. Lett.*, 1982, vol. 21, p. 103.